$B_c^{(*)}$-meson production via the proton-nucleus and the nucleus-nucleus collision modes at the colliders RHIC and LHC

Gu Chen,[1,‡] Chao-Hsi Chang,[2,3,†] and Xing-Gang Wu[4,*]

[1]School of Physics & Electronic Engineering, Guangzhou University, Guangzhou 510006, People's Republic of China
[2]Institute of Theoretical Physics, Chinese Academy of Sciences, P.O.Box 2735, Beijing 100080, People's Republic of China
[3]School of Physical Sciences, University of Chinese Academy of Sciences, Beijing 100049, China
[4]Department of Physics, Chongqing University, Chongqing 401331, People's Republic of China

(Received 30 March 2018; published 21 June 2018)

In the paper, we make a comprehensive study of the hadroproduction of the $B_c(B_c^*)$ meson via the gluon-gluon fusion mechanism at the RHIC and LHC colliders. Total and differential cross sections via the proton-nucleus (p-N) and nucleus-nucleus (N-N) collision modes have been discussed under various collision energies. To compare with those via the proton-proton collision mode at the LHC, we observe that a sizable number of $B_c(B_c^*)$-meson events can also be produced via the p-N and N-N collision modes at the RHIC and LHC. If assuming the spin-triplet B_c^* meson directly decays to the spin-singlet B_c meson with 100% probability, 1.2×10^5 and 4.7×10^5 B_c-meson events can be produced via the p-Au and Au-Au collision modes at the RHIC in one operation year, and 5.8×10^6 and 4.6×10^6 B_c-meson events can be produced via the p-Pb and Pb-Pb collision modes at the LHC in one operation year.

DOI: 10.1103/PhysRevD.97.114022

I. INTRODUCTION

The $(c\bar{b})$-quarkonium is an important system for understanding various aspects of quantum chromodynamics (QCD). It carries flavors explicitly and decays via the weak interaction only, which has a relatively longer lifetime than any other doubly heavy quarkoniums. The masses of the c-quark and the $\bar{b}$-quark as well as the relevant CKM matrix elements happen to cause comparable decay rates for either the constituent c-quark decay channels or the constituent $\bar{b}$-quark decay channels. Those properties make the $(c\bar{b})$-quarkonium (B_c and B_c^* etc) a fruitful "laboratory" for testing the QCD potential models and for understanding the weak decay mechanism of the two heavy flavors simultaneously.

It is known that the behavior of the formation and dissociation of the $(c\bar{c})$-quarkonium (J/ψ etc) in heavy ion collisions offers important information about the quark-gluon plasma (QGP) produced in high-energy heavy ion collisions. From lattice calculations and potential models, the binding energy of the $(c\bar{b})$-quarkonium is greater than that of the $(c\bar{c})$-quarkonium (but lower than that of the $(b\bar{b})$-quarkonium); thus, it is believed that the behavior of the formation and dissociation of the $(c\bar{b})$-quarkonium in high-energy heavy ion collisions will offer more useful information about the QGP to complement those via the formation and dissociation of the $(c\bar{c})$-quarkonium, e.g., the dissociation temperature of the $(c\bar{b})$-quarkonium in the QGP must be higher than that of the $(c\bar{c})$-quarkonium, so the studies on QGP via the $(c\bar{b})$-quarkonium in high-energy heavy ion collisions, paralleled with those via the $(c\bar{c})$-quarkonium, are important and interesting [1]. Aiming this in mind, we think that as a preliminary step, the direct production of the $(c\bar{b})$-quarkonium in high-energy heavy ion collisions should be well understood. In this paper, we shall restrict ourselves to studying the direct production mechanism of the $(c\bar{b})$-quarkonium in high-energy heavy ion collisions.

According to the nonrelativistic quantum chromodynamics (NRQCD) effective theory [2], the $(c\bar{b})$-pair in the quarkonium could be in either the color-singlet state or the color-octet state which can form the measurable color-singlet state by properly grabbing soft gluons or light quarks. In the paper, as a leading-order estimation of the $(c\bar{b})$-quarkonium hadroproduction via the nucleus

‡speecgu@gzhu.edu.cn
†zhangzx@itp.ac.cn
*Corresponding author.
wuxg@cqu.edu.cn

Published by the American Physical Society under the terms of the Creative Commons Attribution 4.0 International license. Further distribution of this work must maintain attribution to the author(s) and the published article's title, journal citation, and DOI. Funded by SCOAP³.

collision modes, we shall concentrate our attention on the color-singlet $B_c(|c\bar{b}[^1S_0]\rangle)$ and $B_c^*(|c\bar{b}[^3S_1]\rangle)$, which are in spin-singlet and spin-triplet states, respectively. The B_c^* meson can decay to the ground state B_c meson with almost 100% possibility via electromagnetic interactions, and the production of B_c^* can be an additional source of the B_c-meson production.

For the production of color-singlet bound-state, the production rates of the B_c meson can be factorized into the convolution of the perturbative short-distance coefficient and the nonperturbative wave function at the origin of the bounding system [3]. Initial theoretical studies on the B_c-meson production at the e^+e^- collider had been given in Refs. [4–6], which stimulated the first experimental search of the B_c meson by collaborations such as OPAL [7], DELPHI [8] and ALEPH [9] at the Large Electron Positron Collider (LEP) [10]. But due to a small production rate and low integrated luminosity accumulated at the LEP-I and LEP-II runs, very few candidate events were observed by those collaborations, so they could not ensure its observation. However, in future high luminosity e^+e^- and ep colliders, such as the International Linear Collider (ILC) [11], the super Z-factory [12,13] and the Large Hadron Electron Collider (LHeC) [14], a sizable number of B_c-meson events may be generated via the electroproduction or photoproduction mechanisms [15–21].

In the same period of time, suggestions for observing the B_c meson at the TEVATRON and the Large Hadron Collider (LHC) were investigated in the literature [22–29]. In 1998, the CDF Collaboration at the TEVATRON reported their first observation of the B_c meson [30] by using the "golden channels" such as the $B_c \to J/\psi$ semileptonic decays [31–33]. This observation was subsequently confirmed by more precise data accumulated at the TEVATRON and the LHC. That experimental progress aroused widespread interest in the B_c meson. Later on, more hadroproduction mechanisms, in addition to the dominant gluon-gluon fusion mechanism, were discussed in the literature [34–37]. Those works culminated in a generator BCVEGPY [38–42], which is now widely accepted by various experimental collaborations for simulating the B_c-meson events at the hadronic colliders.

The ALICE at the LHC and the Star etc. at the RHIC are heavy-ion detectors, which may work in proton-nucleus (p-N) mode or in nucleus-nucleus (N-N) collision mode. Roughly, for the same integrated luminosity, one would expect that 2 or more orders larger cross sections for the B_c-meson production can be achieved via heavy-ion collisions than with the pp collisions. As will be shown later, about 10^6 $B_c^{(*)}$-meson events can be produced in Star or ALICE with their designed luminosity in one operation year. Thus, even considering the direct production mechanisms only, in addition to the pp collision at the LHC, those two operating heavy-ion colliders can hopefully be important plateau for studying the B_c-meson properties as long as the signals can be separated from the background.

At present, the charmonium and bottomonium productions via the p-N or N-N collision mode have been analyzed theoretically [43–48] and experimentally [49–60]. A comparative agreement between the predictions and the measurements have been achieved. Studies on the B_c-meson production via the p-N and N-N collision modes are still at the initial stage, and it is important to study the availability on the $B_c(B_c^*)$-meson production via the p-N and N-N collision modes. The B_c-meson production via heavy-ion collision provides a brand-new perspective insight into the B_c-meson hadroproduction mechanism. It offers a crucial supplement to various aspects of QCD such as to achieve useful insights into the heavy ion structure. The B_c-meson hadroproduction at the RHIC and LHC in the case of p-N or N-N collision at the RHIC and LHC shall be affected by extra effects from the incident nucleus [48,61,62], since the participant nucleon (proton or neutron) are bound in the incident nucleus. Phenomenologically, before collision, the participant partons may lose energy on the way through the nucleus shadowing effect, and after collision the newly produced B_c meson may be destroyed and/or absorbed when it travels through the rest of the nucleus. Moreover, the physical effects emerging in the B_c production are also expected to improve our understanding of the nucleus parton distribution functions.

The remaining parts of the paper are organized as follows. In Sec. II, we focus on the direct production mechanism for the B_c-meson production in Star etc. (RHIC) and in ALICE (LHC) via the dominant gluon-gluon fusion mechanism and present the calculation technology.[1] In Sec. III, numerical results for the production cross sections together with their uncertainties under suitable choices of input parameters are presented, and those for the pp collision mode are also presented for comparison. Section IV is reserved for a summary.

II. CALCULATION TECHNOLOGY

For the leading-order calculation, which is at the α_s^4-order level, the gluon-gluon fusion mechanism via the subprocess, $g + g \to B_c + \bar{c} + b$, provides dominant contribution to the hadroproduction of B_c meson.

As the first step, two heavy quark pairs, $(c\bar{c})$ and $(b\bar{b})$, are produced via hard scattering process, $g + g \to c + \bar{c} + b + \bar{b}$; it is pQCD calculable since the intermediate gluon should be hard enough to form either a $(c\bar{c})$-pair or a $(b\bar{b})$-pair. Then the c-quark and the $\bar{b}$-quark shall be hadronized into the B_c meson, $c + \bar{b} \to B_c$, via a nonperturbative way which can be characterized by the wave function at the origin. The schematic factorization

[1]The B_c-meson production via the extrinsic or intrinsic heavy quark mechanism is in preparation, which is also important and sizable in small and intermediate p_t regions.

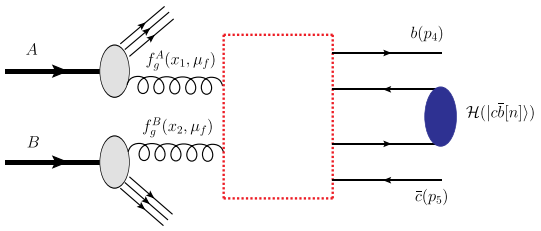

FIG. 1. The schematic factorization picture for the hadronic production of the B_c meson via the gluon-gluon fusion mechanism, where the dashed box stands for the hard interaction kernel, which is perturbatively calculable.

picture for the hadronic production of B_c meson via the gluon-gluon fusion mechanism is shown in Fig. 1.

By using the NRQCD factorization theorem, we can write the total production cross section as

$$d\sigma_{AB\to\mathcal{H}(|c\bar{b}[n]\rangle)+X} = N_A N_B \int dx_1 dx_2 f_g^{\mathrm{A}}(x_1,\mu_f) \times f_g^{\mathrm{B}}(x_2,\mu_f) d\hat{\sigma}_{gg\to|c\bar{b}[n]\rangle+X} \langle\mathcal{O}^{\mathcal{H}}[n]\rangle, \tag{1}$$

where $\langle\mathcal{O}^{\mathcal{H}}[n]\rangle$ is the long-distance matrix element, which is proportional to the inclusive transition probability of the perturbative state $|c\bar{b}[n]\rangle$ into the quarkonium state $\mathcal{H}(|c\bar{b}[n]\rangle)$. The symbols A and B stand for p or N for the incident hadron to be proton or nucleus, respectively. For the nucleus gluon density, we adopt the general approximation that the gluon PDFs in proton and neutron are the same, thus there are overall factors N_A and N_B in the formulae. N_A or N_B is the nuclear number in the incident nucleus, e.g., $N_{\mathrm{Au}} = 197$ for the gold nucleus ($^{197}_{79}$Au), and $N_{\mathrm{Pb}} = 208$ for the lead nucleus ($^{208}_{82}$Pb). The PDFs $f_g^{\mathrm{A}}(x_1,\mu_f)$ and $f_g^{\mathrm{B}}(x_2,\mu_f)$ are gluon PDFs inside the nucleon bound in the nucleus A or B accordingly, which carry the fractions x_1 or x_2 of the nucleon momentum at the factorization scale μ_f. For the pp collision mode, we have $N_A = N_B = 1$, and the PDFs are reduced to the usual gluon PDFs inside the free proton as $f_g^p(x_{1,2},\mu_f)$. Furthermore, we need to consider the collision geometry and the spatial dependence of the shadowing parameterization effect [63,64]. In our present calculation, we shall adopt the nCTEQ15 version [65] as the nucleus PDF, which incorporate those effects into the PDF via global fit of the experimental data.

By ignoring the small spin-splitting effect, the color-singlet S-wave matrix element $\langle\mathcal{O}^{\mathcal{H}}[^1S_0]\rangle = \langle\mathcal{O}^{\mathcal{H}}[^3S_1]\rangle = |R_S(0)|^2/4\pi$, where the radial wavefunction at the origin $|R_S(0)|^2 = 1.642\ \mathrm{GeV}^3$ under the Buchmuller-Tye potential model [66,67]. $d\hat{\sigma}_{gg\to|c\bar{b}[n]\rangle+X}$ is the differential cross section of the hard subprocess,

$$d\hat{\sigma}_{gg\to|c\bar{b}[n]\rangle+X} = \frac{1}{2x_1x_2S_{AB}}\overline{\sum}|\mathcal{M}|^2 d\Phi_m. \tag{2}$$

Here S_{AB} is the center-of-mass energy of the incident hadrons A and B. $\overline{\sum}$ means the averaging over the spin states of the incident gluons and summing over the color and spin of all final particles. $\mathcal{M}$ is the hard scattering amplitude for the subprocess $g(k_1)+g(k_2)\to|(c\bar{b})_{\mathbf{1}}[n]\rangle(p_3)+b(p_4)+\bar{c}(p_5)$. $d\Phi_m$ is the m-body phase space defined as

$$d\Phi_m = (2\pi)^4\delta^4\left(k_1+k_2-\sum_f^m q_f\right)\prod_{f=1}^n \frac{d\vec{q}_f}{(2\pi)^3 2q_f^0}. \tag{3}$$

We adopt the generator BCVEGPY to deal with the hard scattering amplitude and the phase space.

III. NUMERICAL RESULTS

A. Input parameters

As for the heavy quark masses, we take $m_c = 1.5$ GeV and $m_b = 4.9$ GeV. To ensure the gauge invariance of the hard scattering amplitude, the B_c-meson mass is the sum of the two constituent quark masses, $M_{B_c} = m_b + m_c$. The renormalization scale and the factorization scale are set to be the same and are taken as the transverse mass of the B_c meson, i.e., $\mu_R = \mu_f = M_t = \sqrt{M_{B_c}^2 + p_t^2}$.

In the p-N and N-N collision modes, the nucleus beam energy per nucleon E_{N} is related to the proton beam energy E_p and the charge-to-mass ratio of the incoming nucleus Z/N_A, $E_{\mathrm{N}} = E_p Z/N_A$ [48].

At the LHC, the collision energy for its pp collision mode is $\sqrt{S_{pp}} = 13$ TeV and the proton beam energy $E_p = 6.5$ TeV; the collision energy for its p-Pb collision model is $\sqrt{S_{p\mathrm{Pb}}} = \sqrt{4E_pE_{\mathrm{Pb}}} = 8.16$ TeV; the collision energy for its Pb-Pb collision mode is $\sqrt{S_{\mathrm{PbPb}}} = 5.02$ TeV. At the RHIC, the collision energy is taken as $\sqrt{S_{p\mathrm{Au}}} = 0.2$ TeV for the p-Au collision and $\sqrt{S_{\mathrm{AuAu}}} = 0.2$ TeV for the Au-Au collision, respectively.

B. Basic results

Total cross sections for the B_c-meson production under various hadron-hadron collision modes via the gluon-gluon fusion mechanism are presented in Table I. The production cross sections of $B_c^{(*)}$ in the p-N and N-N collision modes are much larger than that of the pp collision, due to the large nuclear number in the Pb nucleus. For the case of production at the LHC, the relative importance of the total cross sections under different collision modes is $\sigma_{pp}|_{\sqrt{S}=13\ \mathrm{TeV}} : \sigma_{p\mathrm{Pb}}|_{\sqrt{S}=8.16\ \mathrm{TeV}} : \sigma_{\mathrm{PbPb}}|_{\sqrt{S}=5.02\ \mathrm{TeV}} = 1:78:8736$, where the contributions from B_c and B_c^* have been

TABLE I. Total cross sections (in unit: nb) for the $B_c^{(*)}$-meson production via the gluon-gluon fusion mechanism at the RHIC and the LHC, respectively. Typical collision energies for various collision modes are adopted. As a comparison, we present the cross sections for the two color-octet $|({}^1S_0)_{\mathbf{8}}g\rangle$ and $|({}^3S_1)_{\mathbf{8}}g\rangle$ by using the same color-octet matrix elements as those of Ref. [37].

	RHIC		LHC		
	p-Au (0.2 TeV)	Au-Au (0.2 TeV)	pp (13 TeV)	p-Pb (8.16 TeV)	Pb-Pb (5.02 TeV)
σ_{B_c} (nb)	8.19	1.76×10^3	4.24×10^1	3.29×10^3	3.69×10^5
$\sigma_{B_c^*}$ (nb)	1.93×10^1	4.15×10^3	1.05×10^2	8.26×10^3	9.21×10^5
$\sigma_{\lvert({}^1S_0)_{\mathbf{8}}g\rangle}$ (nb)	1.82×10^{-1}	3.94×10^1	7.89×10^{-1}	5.96×10^1	6.83×10^3
$\sigma_{\lvert({}^3S_1)_{\mathbf{8}}g\rangle}$ (nb)	8.36×10^{-1}	1.83×10^2	3.40	2.55×10^2	2.90×10^4

summed up. As required, due to the shadowing effect, this ratio is smaller than the simple estimation of $1 : N_{\rm Pb} : N_{\rm Pb}^2$.

As a useful reference, we also present the simple prediction on the color-octet states $|({}^1S_0)_{\mathbf{8}}g\rangle$ and $|({}^3S_1)_{\mathbf{8}}g\rangle$ at the RHIC and the LHC in Table I, in which the same color-octet matrix elements as those of Ref. [37] are adopted. Table I shows that the color-octet contribution are about $2\% \sim 4\%$ of the color-singlet S-wave states for both the p-N and N-N collisions at the RHIC and the LHC. Thus in the following discussions, we shall concentrate on the color-singlet S-wave production.[2]

To estimate how many B_c-meson events can be produced at the RHIC and LHC, we sum up the $B_c({}^1S_0)$ and $B_c^*({}^3S_1)$ contributions together and adopt the designed luminosity of RHIC and LHC [68] to do the estimation. For convenience, we use a short notation to express the integrated luminosity per operation year,[3] i.e., $\mathcal{L}_{\rm M}^{\rm R(L)}$, where R(L) stands for RHIC (LHC), and the subscript M represents the mentioned collision modes pp, p-N, and N-N, respectively.

At the RHIC, the designed luminosities for the p-Au and the Au-Au collision modes are 4.5×10^{29} cm^{-2} s^{-1} and 8.0×10^{27} cm^{-2} s^{-1}, and the integrated luminosities are $\mathcal{L}_{p\rm Au}^{\rm R} = 4.5$ pb^{-1} and $\mathcal{L}_{\rm AuAu}^{\rm R} = 80$ nb^{-1}, respectively. Consequently, we shall have 1.2×10^5 and 4.7×10^5 B_c-meson events to be generated in p-Au and Au-Au collisions at the RHIC in one operation year.

At the LHC, the designed luminosities for the pp, p-Pb and the Pb-Pb collision modes are 5.0×10^{33} cm^{-2} s^{-1}, 5.0×10^{29} cm^{-2} s^{-1} and 3.6×10^{27} cm^{-2} s^{-1} and the integrated luminosities are $\mathcal{L}_{pp}^{\rm L} = 50$ fb^{-1}, $\mathcal{L}_{p\rm Pb}^{\rm L} = 0.5$ pb^{-1} and $\mathcal{L}_{\rm PbPb}^{\rm L} = 3.6$ nb^{-1}, respectively. Consequently, we shall have 7.4×10^9, 5.8×10^6 and 4.6×10^6 B_c-meson events to be generated in pp, p-Pb and Pb-Pb collisions at the LHC in one operation year.

Thus, Table I shows that in addition to the pp collision mode at the LHC, sizable B_c-meson events can also be produced at both the RHIC and the LHC via the p-N and N-N collision modes. The p-N and N-N collision modes should also be capable of comprehensive studies on various aspects of B_c-meson physics.

C. Differential distributions of the $B_c(B_c^*)$-meson production via the p-N and N-N collision modes

We present the p_t distributions of the $B_c^{(*)}$-meson productions at the RHIC and the LHC via the p-N and the N-N collision modes in Figs. 2 and 3. The p_t distributions for the p-N and the N-N collision modes at the RHIC and the LHC are close in shape, which shall first increase and then decreases quickly with the increment of p_t.

We present the rapidity (y) and pseudo-rapidity (y_p) distributions of the $B_c^{(*)}$-meson productions at the RHIC and the LHC via the p-N and N-N collision modes in

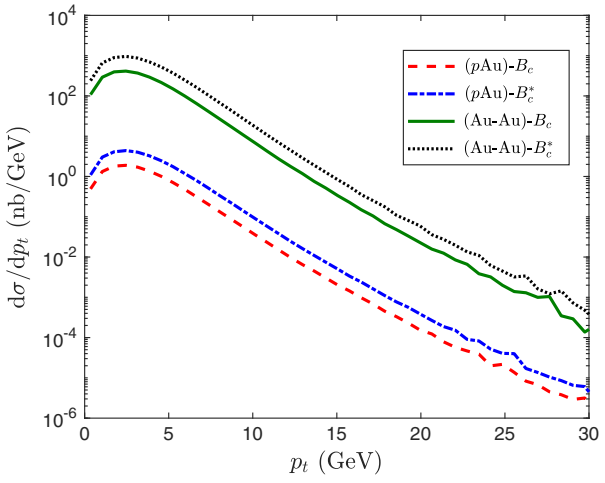

FIG. 2. The p_t-distributions of the $B_c^{(*)}$-meson production via the p-Au and Au-Au collision modes at the RHIC. $\sqrt{S_{p\rm Au}} = 200$ GeV and $\sqrt{S_{\rm AuAu}} = 200$ GeV.

[2]The color-octet production cross sections depend heavily on the magnitude of the color-octet matrix elements. The color-octet components are sizable in comparison to the color-singlet P-wave states, thus they should be taken into consideration when discussing the production of the P-wave states. A detailed discussion on the production of the P-wave states together with those two color-octet S-wave states is in preparation.

[3]At the RHIC, one operation year equals 10^7 s for p-N and N-N collisions. At the LHC, one operation year equals 10^7 s for pp-collision and 10^6 s for p-N and N-N collisions [69,70].

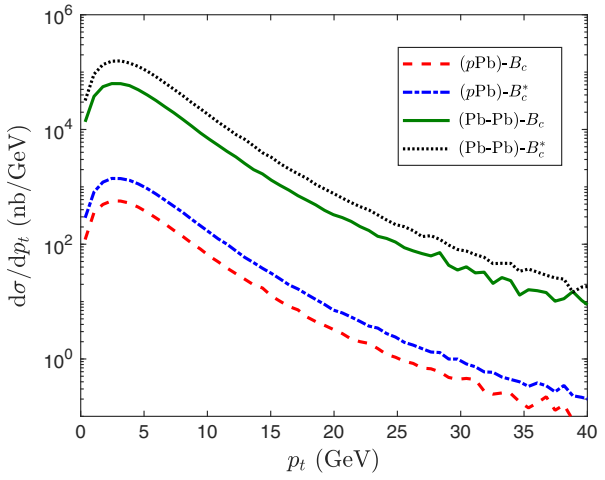

FIG. 3. The p_t-distribution of the $B_c^{(*)}$-meson production via the p-Pb and Pb-Pb collision modes at the LHC. $\sqrt{S_{p\mathrm{Pb}}} = 8.16$ TeV and $\sqrt{S_{\mathrm{PbPb}}} = 5.02$ TeV.

Figs. 4–7. Those distributions are asymmetric for the p-Au and p-Pb collision modes, which are more obvious for the p-Pb collision mode due to the fact that much more small x events appearing at the LHC, thus the differences between the proton gluon PDF and the nucleus gluon PDF are greatly amplified. There are plateau for the rapidity and pseudo-rapidity distributions with $|y| \leq 2$ or $|y_p| \leq 2$ at the RHIC for the p-Au and Au-Au collision modes. At the LHC, such plateau become broader, which change to $|y| \leq 4$ or $|y_p| \leq 4$ for the p-Pb and Pb-Pb collision modes, respectively.

In a high-energy collider, the B_c meson events with a small p_t and/or a large rapidity y, indicating they are moving close to the beam direction, cannot be detected by the detectors directly, so those events cannot be utilized for experimental studies in common cases. Considering the

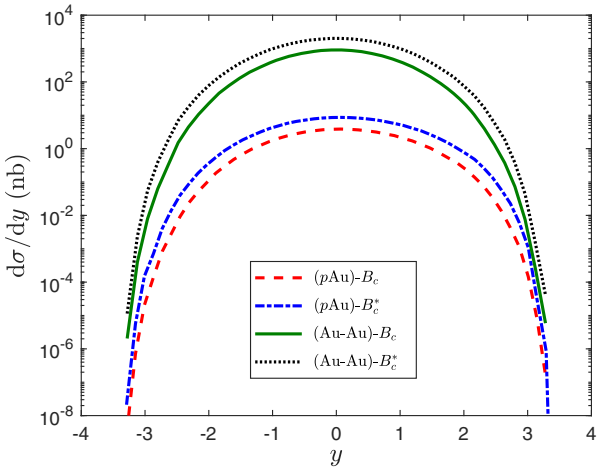

FIG. 4. The y-distribution of the $B_c^{(*)}$-meson production via the p-Au and Au-Au collision modes at the RHIC. $\sqrt{S_{p\mathrm{Au}}} = 200$ GeV and $\sqrt{S_{\mathrm{AuAu}}} = 200$ GeV.

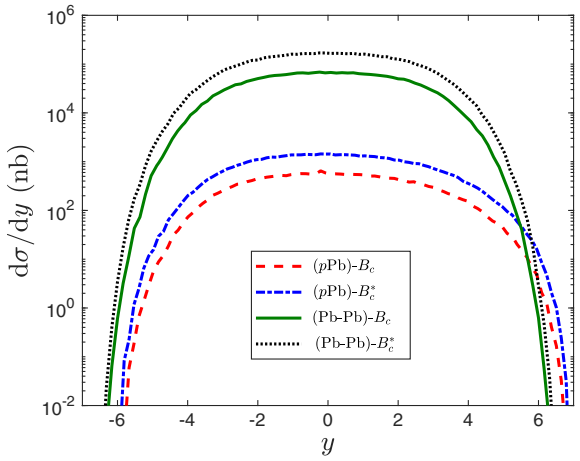

FIG. 5. The y-distribution of the $B_c^{(*)}$-meson production via the p-Pb and Pb-Pb collision modes at the LHC. $\sqrt{S_{p\mathrm{Pb}}} = 8.16$ TeV and $\sqrt{S_{\mathrm{PbPb}}} = 5.02$ TeV.

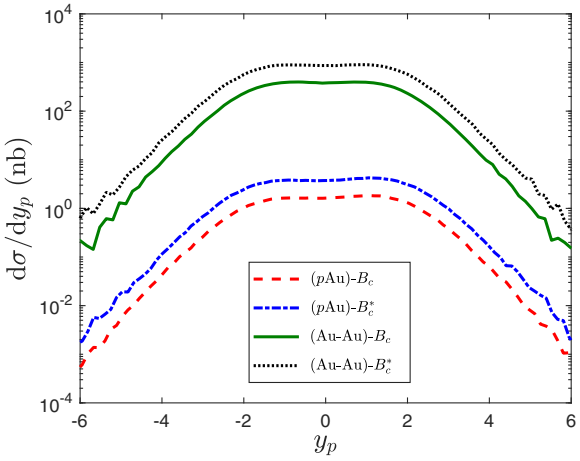

FIG. 6. The y_p-distribution of the $B_c^{(*)}$-meson production via the p-Au and Au-Au collision modes at the RHIC. $\sqrt{S_{p\mathrm{Au}}} = 200$ GeV and $\sqrt{S_{\mathrm{AuAu}}} = 200$ GeV.

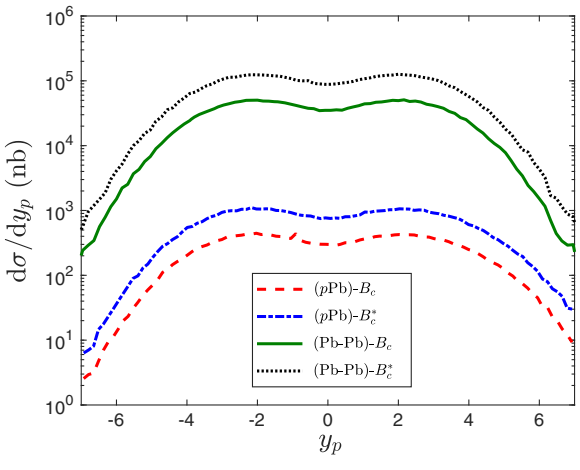

FIG. 7. The y_p-distribution of the $B_c^{(*)}$-meson production via the p-Pb and Pb-Pb collision modes at the LHC. $\sqrt{S_{p\mathrm{Pb}}} = 8.16$ TeV and $\sqrt{S_{\mathrm{PbPb}}} = 5.02$ TeV.

TABLE II. Total cross sections (in unit: nb) of the $B_c^{(*)}$-meson production under various transverse momentum cuts at the RHIC and the LHC via p-N and N-N collision modes, respectively.

	RHIC				LHC			
	p-Au (0.2 TeV)		Au-Au (0.2 TeV)		p-Pb (8.16 TeV)		Pb-Pb (5.02 TeV)	
	σ_{B_c} (nb)	$\sigma_{B_c^*}$ (nb)	σ_{B_c} (nb)	$\sigma_{B_c^*}$ (nb)	σ_{B_c} (nb)	$\sigma_{B_c^*}$ (nb)	σ_{B_c} (nb)	$\sigma_{B_c^*}$ (nb)
$p_t \geq 2$ GeV	5.82	1.39×10^1	1.25×10^3	2.98×10^3	2.72×10^3	6.86×10^3	3.01×10^5	7.62×10^5
$p_t \geq 4$ GeV	1.42	5.93	5.08×10^2	1.25×10^3	1.60×10^3	4.08×10^3	1.75×10^5	4.51×10^5
$p_t \geq 6$ GeV	7.58×10^{-1}	1.91	1.54×10^2	3.84×10^2	8.02×10^2	2.06×10^3	8.90×10^4	2.26×10^5

TABLE III. Total cross sections (in unit: nb) of the $B_c^{(*)}$-meson production under various rapidity cuts at the RHIC and the LHC via p-N and N-N collision modes, respectively.

	RHIC				LHC			
	p-Au (0.2 TeV)		Au-Au (0.2 TeV)		p-Pb (8.16 TeV)		Pb-Pb (5.02 TeV)	
	σ_{B_c} (nb)	$\sigma_{B_c^*}$ (nb)	σ_{B_c} (nb)	$\sigma_{B_c^*}$ (nb)	σ_{B_c} (nb)	$\sigma_{B_c^*}$ (nb)	σ_{B_c} (nb)	$\sigma_{B_c^*}$ (nb)
$\lvert y\rvert \leq 1$	6.31	1.44×10^1	1.44×10^3	3.26×10^3	1.10×10^3	2.75×10^3	1.30×10^5	3.32×10^5
$\lvert y\rvert \leq 2$	8.09	1.90×10^1	1.75×10^3	4.11×10^3	2.09×10^3	5.12×10^3	2.46×10^5	6.12×10^5
$\lvert y\rvert \leq 3$	8.17	1.93×10^1	1.76×10^3	4.15×10^3	2.81×10^3	6.96×10^3	3.27×10^5	8.19×10^5

detectors abilities and in order to offer experimental references, we try various cuts accordingly in the estimate of the B_c meson production.

We present the cross sections under typical cuts $p_t \geq 2$ GeV, $p_t \geq 4$ GeV, and $p_t \geq 6$ GeV in Table II. If taking the p_t cut equals 2 GeV (6 GeV), the total cross section shall be reduced by ∼17% (∼75%) for both the p-Pb and Pb-Pb collision modes at the LHC, and by ∼28% (∼90%) for both the p-Au and Au-Au collision modes at the RHIC. Similarly, we present the cross sections for three typical rapidity cuts, $|y| \leq 1$, $|y| \leq 2$, and $|y| \leq 3$, in Table III.

D. Uncertainties from different choices of the heavy quark masses and renormalization scale

In this subsection, we discuss the uncertainties from different choices of heavy quark mass and the renormalization scale.

To estimate the uncertainties from the heavy quark masses m_c and m_b, we take $m_c = 1.50 \pm 0.10$ GeV and $m_b = 4.9 \pm 0.20$ GeV. When the quark masses are changed, the mass of the B_c meson shall be alternated accordingly to ensure $M_{B_c} = m_b + m_c$. We present the results in Tables IV and V. Those two tables show that the total cross section depends heavily on the value of the c-quark or the b-quark mass, which decreases with the increment of the quark mass and is more sensitive to the c-quark mass. By summing the spin-singlet and spin-triplet contributions together, Table IV shows that by taking $\Delta m_c = \pm 0.1$ GeV, the cross section shall be changed by $[-20\%, +34\%]$ for the RHIC and by $[-17\%, 27\%]$ for the LHC; Table V shows that by taking $\Delta m_b = \pm 0.2$ GeV, the total cross section shall be changed by $[-15\%, +26\%]$ for the RHIC and by $[-11\%, +16\%]$ for the LHC.

As an estimation of renormalization scale dependence, we take three typical scales to calculate the total cross section. The results are presented in Table VI. In addition to the transverse mass M_t, we take another two choices $\mu_R = \sqrt{\hat{s}}/2$ and $\mu_R = \sqrt{\hat{s}}$ to do the estimation, where $\sqrt{\hat{s}}$ is the center-of-mass energy of the subprocess.

TABLE IV. Total cross sections (in unit: nb) of the $B_c^{(*)}$-meson production with different c-quark masses at the RHIC and the LHC via p-N and N-N collision modes, respectively.

	RHIC				LHC			
	p-Au (0.2 TeV)		Au-Au (0.2 TeV)		p-Pb (8.16 TeV)		Pb-Pb (5.02 TeV)	
m_c	σ_{B_c} (nb)	$\sigma_{B_c^*}$ (nb)	σ_{B_c} (nb)	$\sigma_{B_c^*}$ (nb)	σ_{B_c} (nb)	$\sigma_{B_c^*}$ (nb)	σ_{B_c} (nb)	$\sigma_{B_c^*}$ (nb)
1.4 GeV	1.06×10^1	2.57×10^1	2.29×10^3	5.55×10^3	4.05×10^3	1.05×10^4	4.53×10^5	1.15×10^6
1.5 GeV	8.19	1.93×10^1	1.76×10^3	4.15×10^3	3.29×10^3	8.26×10^3	3.69×10^5	9.21×10^5
1.6 GeV	6.42	1.47×10^1	1.38×10^3	3.14×10^3	2.75×10^3	6.69×10^3	3.04×10^5	7.44×10^5

TABLE V. Total cross sections (in unit: nb) of the $B_c^{(*)}$-meson production with different b-quark masses at the RHIC and the LHC via p-N and N-N collision modes, respectively.

	RHIC				LHC			
	p-Au (0.2 TeV)		Au-Au (0.2 TeV)		p-Pb (8.16 TeV)		Pb-Pb (5.02 TeV)	
m_b	σ_{B_c} (nb)	$\sigma_{B_c^*}$ (nb)	σ_{B_c} (nb)	$\sigma_{B_c^*}$ (nb)	σ_{B_c} (nb)	$\sigma_{B_c^*}$ (nb)	σ_{B_c} (nb)	$\sigma_{B_c^*}$ (nb)
4.7 GeV	1.03×10^1	2.38×10^1	2.23×10^3	5.14×10^3	3.83×10^3	9.40×10^3	4.26×10^5	1.04×10^6
4.9 GeV	8.19	1.93×10^1	1.76×10^3	4.15×10^3	3.29×10^3	8.26×10^3	3.69×10^5	9.21×10^5
5.1 GeV	6.55	1.57×10^1	1.40×10^3	3.35×10^3	2.86×10^3	7.29×10^3	3.19×10^5	8.12×10^5

TABLE VI. Total cross sections (in unit: nb) of $B_c^{(*)}$-meson production with three typical choices of renormalization scale μ_R at RHIC and LHC via p-N and N-N collision modes, respectively.

	RHIC				LHC			
	p-Au (0.2 TeV)		Au-Au (0.2 TeV)		p-Pb (8.16 TeV)		Pb-Pb (5.02 TeV)	
μ_R	σ_{B_c} (nb)	$\sigma_{B_c^*}$ (nb)	σ_{B_c} (nb)	$\sigma_{B_c^*}$ (nb)	σ_{B_c} (nb)	$\sigma_{B_c^*}$ (nb)	σ_{B_c} (nb)	$\sigma_{B_c^*}$ (nb)
$\sqrt{\hat{s}}$	2.32	5.34	4.95×10^2	1.12×10^3	1.83×10^3	4.51×10^3	1.94×10^5	4.77×10^5
$\sqrt{\hat{s}}/2$	5.29	1.21×10^1	1.14×10^3	2.61×10^3	2.46×10^3	6.06×10^3	2.69×10^5	6.58×10^5
M_t	8.19	1.93×10^1	1.76×10^3	4.15×10^3	3.29×10^3	8.26×10^3	3.69×10^5	9.21×10^5

At the tree level, there is large scale uncertainty. By summing the spin-singlet and spin-triplet contributions together, the uncertainties are ∼70% for the p-Au and Au-Au collision modes at the RHIC, which change down to ∼45% for the p-Pb and Pb-Pb collision modes at the LHC. To suppress the scale uncertainty, it is helpful to finish a next-to-leading-order calculation. In fact, even if we have finished such a high-order calculation, we still need a proper scale-setting approach such that to achieve a scheme-and-scale independent prediction at lower orders [71,72].

IV. SUMMARY

By taking the gluon-gluon fusion production mechanism into consideration, we have performed a detailed discussion on the $B_c(B_c^*)$-meson production via the p-N and N-N collision modes at the RHIC and LHC, respectively. It is found that sizable number of B_c-meson events may be produced at the RHIC and LHC via the p-N and N-N collision modes. For instance, if assuming all the spin-triplet B_c^*-meson decay to the spin-singlet B_c meson with 100% probability, 1.2×10^5 and 4.7×10^5 B_c-meson events shall be produced via the p-Au and Au-Au collision modes at the RHIC in one operation year; and 5.8×10^6 and 4.6×10^6 B_c-meson events shall be produced via the p-Pb and Pb-Pb collision modes at the LHC in one operation year.

Differential distributions for various collision modes have been presented in Figs. 2–7. The p_t distributions are close in shape to each other, which decrease quickly in large p_t region. The rapidity and pseudo-rapidity distributions in the p-N collision mode are asymmetric in certain manner, which become more and more obvious at the LHC due to more small x-events appear and the differences between the gluon components in proton and in nucleus shall be greatly amplified. There are plateau in the rapidity and pseudo-rapidity distributions for the production of the $B_c(B_c^*)$ meson via various heavy-ion collision modes. Those plateau become broader and broader with increasing collision energies among the incident hadrons, e.g., at the RHIC the plateau appear within the region of $|y| \leq 2$ or $|y_p| \leq 2$, which change to $|y| \leq 4$ or $|y_p| \leq 4$ for the case of LHC.

There are large uncertainties from the value of the heavy quark masses and the chosen renormalization scale, which could be suppressed by including high-order terms.

In summary for the productions of the $B_c(B_c^*)$ meson at the RHIC, we obtain

$$\sigma_{B_c}^{p\mathrm{Au}} = 8.19^{+2.39+2.11}_{-1.77-1.64}\ \mathrm{nb}, \tag{4}$$

$$\sigma_{B_c^*}^{p\mathrm{Au}} = 19.3^{+6.35+4.51}_{-4.65-3.62}\ \mathrm{nb}, \tag{5}$$

$$\sigma_{B_c}^{\mathrm{AuAu}} = 1.76^{+0.52+0.47}_{-0.38-0.36}\ \mu\mathrm{b}, \tag{6}$$

$$\sigma_{B_c^*}^{\mathrm{AuAu}} = 4.15^{+1.41+0.99}_{-1.01-0.79}\ \mu\mathrm{b}; \tag{7}$$

and for the production at the LHC, we obtain

$$\sigma_{B_c}^{p\mathrm{Pb}} = 3.29^{+0.76+0.54}_{-0.55-0.44}\ \mu\mathrm{b}, \tag{8}$$

$$\sigma_{B_c^*}^{p\mathrm{Pb}} = 8.26^{+2.22+1.14}_{-1.57-0.97}\ \mu\mathrm{b}, \tag{9}$$

$$\sigma_{B_c}^{\mathrm{PbPb}} = (3.69 \times 10^2)^{+8.35\times10^1+5.69\times10^1}_{-6.49\times10^1-5.01\times10^1}\ \mu\mathrm{b}, \tag{10}$$

$$\sigma_{B_c^*}^{\mathrm{PbPb}} = (9.21 \times 10^2)^{+2.31\times10^2+1.22\times10^2}_{-1.78\times10^2-1.09\times10^2}\ \mu\mathrm{b}. \tag{11}$$

Here the first error is for $\Delta m_c = \pm 0.1$ GeV and the second error is for $\Delta m_b = \pm 0.2$ GeV, and no p_t and rapidity cuts are taken in those predictions.

We have shown that sizable number of B_c-meson events can be produced at both the RHIC and LHC via the p-N and N-N collision modes. On one hand, it indicates that one may study the B_c-meson properties by using more collision modes other than the usually considered pp collision mode. On the other hand, it shows that to study the QGP via the signals of the B_c meson is feasible. Moreover the information shall be useful for testing the nucleus PDFs, especially to test the shadowing effects etc within the nucleus. At present, our discussions are concentrated on the S-wave $(c\bar{b})$-quarkonium states and on the dominant direct gluon-gluon fusion production mechanism, the studies on the production of higher excited $(c\bar{b})$-quarkonium states and on different production mechanisms, such as intrinsic charm or extrinsic charm mechanism, are also important.

ACKNOWLEDGMENTS

We would like to thank Hua-Yong Han for helpful discussions. This work was supported in part by the Natural Science Foundation of China under Grants No. 11605029, No. 11675239, No. 11625520, and No. 11535002, the science project of colleges and universities directly under the Guangzhou Education Bureau under Grant No. 1201630158, and The Foundation for Fostering the Scientific and Technical Innovation of Guangzhou University.

[1] N.-b. Chang *et al.*, Physics perspectives of heavy-ion collisions at very high energy, Sci. China Phys. Mech. Astron. **59**, 621001 (2016).
[2] G. T. Bodwin, E. Braaten, and G. P. Lepage, Rigorous QCD analysis of inclusive annihilation and production of heavy quarkonium, Phys. Rev. D **51**, 1125 (1995).
[3] C. H. Chang, HadronicpProduction of J/ψ associated with a gluon, Nucl. Phys. **B172**, 425 (1980).
[4] C. H. Chang and Y. Q. Chen, The B_c and anti-B_c mesons accessible to experiments through Z^0 bosons decay, Phys. Lett. B **284**, 127 (1992).
[5] C. H. Chang and Y. Q. Chen, The production of B_c or anti-B_c meson associated with two heavy quark jets in Z^0 boson decay, Phys. Rev. D **46**, 3845 (1992).
[6] V. V. Kiselev, A. K. Likhoded, and M. V. Shevlyagin, B_c and b anti-b c anti-c at the Z^0 boson pole, Z. Phys. C **63**, 77 (1994).
[7] K. Ackerstaff *et al.* (OPAL Collaboration), Search for the B_c meson in hadronic Z^0 decays, Phys. Lett. B **420**, 157 (1998).
[8] P. Abreu *et al.* (DELPHI Collaboration), Search for the B(c) meson, Phys. Lett. B **398**, 207 (1997).
[9] R. Barate *et al.* (ALEPH Collaboration), Search for the B_c meson in hadronic Z decays, Phys. Lett. B **402**, 213 (1997).
[10] R. Aβmann, M. Lamont, and S. Myers, A brief history of the LEP collider, Nucl. Phys. Proc. Suppl. B **109**, 17 (2002).
[11] A. Djouadi *et al.* (ILC Collaboration), International Linear Collider Reference Design Report Volume 2: Physics at the ILC, arXiv:0709.1893.
[12] J. Erler, S. Heinemeyer, W. Hollik, G. Weiglein, and P. M. Zerwas, Physics impact of GigaZ, Phys. Lett. B **486**, 125 (2000).
[13] J. P. Ma and Z. X. Zhang (The Super Z-factory Group), Z-Factory physics, Sci. China: Phys. Mech. Astron. **53**, 1947 (2010).
[14] J. L. A. Fernandez *et al.* (LHeC Study Group), A large hadron electron collider at CERN: Report on the physics and design concepts for machine and detector, J. Phys. G **39**, 075001 (2012).
[15] C. H. Chang, J. X. Wang, and X. G. Wu, Production of a Heavy Quarkonium with a Photon or via ISR at Z Peak in e^+e^- Collider, Sci. China Phys. Mech. Astron. **53**, 2031 (2010).
[16] Z. Yang, X. G. Wu, G. Chen, Q. L. Liao, and J. W. Zhang, B_c Meson Production around the Z^0 Peak at a high luminosity e^+e^- collider, Phys. Rev. D **85**, 094015 (2012).
[17] Z. Yang, X. G. Wu, and X. Y. Wang, BEEC: An event generator for simulating the B_c meson production at an e^+e^- collider, Comput. Phys. Commun. **184**, 2848 (2013).
[18] Z. Sun, X. G. Wu, G. Chen, J. Jiang, and Z. Yang, Heavy quarkonium production through the semi-exclusive e^+e^- annihilation channels round the Z^0 peak, Phys. Rev. D **87**, 114008 (2013).
[19] X. C. Zheng, C. H. Chang, and Z. Pan, Production of doubly heavy-flavored hadrons at e^+e^- colliders, Phys. Rev. D **93**, 034019 (2016).
[20] X. C. Zheng, C. H. Chang, T. F. Feng, and Z. Pan, NLO QCD corrections to $B_c(B_c^*)$ production around the Z pole at an e^+e^- collider, Sci. China Phys. Mech. Astron. **61**, 031012 (2018).
[21] H. Y. Bi, R. Y. Zhang, H. Y. Han, Y. Jiang, and X. G. Wu, Photoproduction of the $B_c^{(*)}$ meson at the LHeC, Phys. Rev. D **95**, 034019 (2017).
[22] C. H. Chang and Y. Q. Chen, The hadronic production of the B_c meson at Tevatron, CERN LHC and SSC, Phys. Rev. D **48**, 4086 (1993).
[23] C. H. Chang, Y. Q. Chen, G. P. Han, and H. T. Jiang, On hadronic production of the B_c meson, Phys. Lett. B **364**, 78 (1995).
[24] K. Kolodziej, A. Leike, and R. Ruckl, Production of B_c mesons in hadronic collisions, Phys. Lett. B **355**, 337 (1995).
[25] A. V. Berezhnoy, A. K. Likhoded, and M. V. Shevlyagin, Hadronic production of B_c mesons, Phys. At. Nucl. **58**, 672 (1995).

[26] C. H. Chang, Y. Q. Chen, and R. J. Oakes, Comparative study of the hadronic production of B_c mesons, Phys. Rev. D **54**, 4344 (1996).

[27] A. V. Berezhnoy, V. V. Kiselev, and A. K. Likhoded, Hadronic production of S and P wave states of anti-b c quarkonium, Z. Phys. A **356**, 79 (1996).

[28] S. P. Baranov, Semiperturbative and nonperturbative production of hadrons with two heavy flavors, Phys. Rev. D **56**, 3046 (1997).

[29] S. P. Baranov, Pair production of $B_c^{(*)}$ mesons in pp and $\gamma\gamma$ collisions, Phys. Rev. D **55**, 2756 (1997).

[30] F. Abe *et al.* (CDF Collaboration), Observation of the B_c Meson in $p\bar{p}$ Collisions at $\sqrt{s} = 1.8$ TeV, Phys. Rev. Lett. **81**, 2432 (1998).

[31] M. Lusignoli and M. Masetti, B(c) decays, Z. Phys. C **51**, 549 (1991).

[32] C. H. Chang and Y. Q. Chen, The decays of B(c) meson, Phys. Rev. D **49**, 3399 (1994).

[33] D. Scora and N. Isgur, Semileptonic meson decays in the quark model: An update, Phys. Rev. D **52**, 2783 (1995).

[34] C. H. Chang and X. G. Wu, Uncertainties in estimating hadronic production of the meson B_c and comparisons between TEVATRON and LHC, Eur. Phys. J. C **38**, 267 (2004).

[35] C. H. Chang, J. X. Wang, and X. G. Wu, Hadronic production of the P-wave excited B_c -states (B*cJ, $L = 1$), Phys. Rev. D **70**, 114019 (2004).

[36] C. H. Chang, C. F. Qiao, J. X. Wang, and X. G. Wu, Hadronic production of $B_c(B_c^*)$ meson induced by the heavy quarks inside the collision hadrons, Phys. Rev. D **72**, 114009 (2005).

[37] C. H. Chang, C. F. Qiao, J. X. Wang, and X. G. Wu, The Color-octet contributions to P-wave B_c meson hadroproduction, Phys. Rev. D **71**, 074012 (2005).

[38] C. H. Chang, X. Y. Wang, and X. G. Wu, BCVEGPY2.2: A newly upgraded version for hadronic production of the meson Bc and its excited states, Comput. Phys. Commun. **197**, 335 (2015).

[39] C. H. Chang, C. Driouichi, P. Eerola, and X. G. Wu, BCVEGPY: An event generator for hadronic production of the B_c meson, Comput. Phys. Commun. **159**, 192 (2004).

[40] C. H. Chang, J. X. Wang, and X. G. Wu, BCVEGPY2.0: A upgrade version of the generator BCVEGPY with an addendum about hadroproduction of the P-wave B(c) states, Comput. Phys. Commun. **174**, 241 (2006).

[41] C. H. Chang, J. X. Wang, and X. G. Wu, An upgraded version of the generator BCVEGPY2.0 for hadronic production of B(c)meson and its excited states, Comput. Phys. Commun. **175**, 624 (2006).

[42] X. G. Wu, BCVEGPY and GENXICC for the hadronic production of the doubly heavy mesons and baryons, J. Phys. Conf. Ser. **523**, 012042 (2014).

[43] F. Arleo and S. Peigne, Heavy-quarkonium suppression in p-A collisions from parton energy loss in cold QCD matter, High Energy Phys. Nucl. Phys. **2013** (2013) 122.

[44] H. Fujii and K. Watanabe, Heavy quark pair production in high energy pA collisions: Quarkonium, Nucl. Phys. **A915**, 1 (2013).

[45] Y. Q. Ma, R. Venugopalan, and H. F. Zhang, J/ψ production and suppression in high energy proton-nucleus collisions, Phys. Rev. D **92**, 071901 (2015).

[46] B. Duclou, T. Lappi, and H. Mntysaari, Forward J/ψ production in proton-nucleus collisions at high energy, Phys. Rev. D **91**, 114005 (2015).

[47] J. P. Lansberg and H. S. Shao, Towards an automated tool to evaluate the impact of the nuclear modification of the gluon density on quarkonium, D and B meson production in proton nucleus collisions, Eur. Phys. J. C **77**, 1 (2017).

[48] R. Vogt, Cold nuclear matter effects on J/ψ and Υ production at the LHC, Phys. Rev. C **81**, 044903 (2010).

[49] A. Adare *et al.* (PHENIX Collaboration), Nuclear Modification of η_c, and J/ψ Production in d + Au Collisions at $\sqrt{s_{\rm NN}} = 200$ GeV, Phys. Rev. Lett. **111**, 202301 (2013).

[50] B. B. Abelev *et al.* (ALICE Collaboration), J/ψ production and nuclear effects in p-Pb collisions at $\sqrt{s_{\rm NN}} = 5.02$ TeV, J. High Energy Phys. 02 (2014) 073.

[51] R. Aaij *et al.* (LHCb Collaboration), Study of J/ψ production and cold nuclear matter effects in pPb collisions at $\sqrt{s_{\rm NN}} = 5$ TeV, J. High Energy Phys. 02 (2014) 072.

[52] B. B. Abelev *et al.* (ALICE Collaboration), Suppression of $\psi(2S)$ production in p-Pb collisions at $\sqrt{s_{\rm NN}} = 5.02$ TeV, J. High Energy Phys. 12 (2014) 073.

[53] J. Adam *et al.* (ALICE Collaboration), Rapidity and transverse-momentum dependence of the inclusive J/ψ nuclear modification factor in p-Pb collisions at $\sqrt{s_{\rm NN}} = 5.02$ TeV, J. High Energy Phys. 06 (2015) 055.

[54] J. Adam *et al.* (ALICE Collaboration), Centrality dependence of inclusive J/ψ production in p-Pb collisions at $\sqrt{s_{\rm NN}} = 5.02$ TeV, J. High Energy Phys. 11 (2015) 127.

[55] G. Aad *et al.* (ATLAS Collaboration), Measurement of differential J/ψ production cross sections and forward-backward ratios in p + Pb collisions with the ATLAS detector, Phys. Rev. C **92**, 034904 (2015).

[56] R. Aaij *et al.* (LHCb Collaboration), Study of $\psi(2S)$ production and cold nuclear matter effects in p-Pb collisions at $\sqrt{s_{\rm NN}} = 5$ TeV, J. High Energy Phys. 03 (2016) 133.

[57] J. Adam *et al.* (ALICE Collaboration), Centrality dependence of $\psi(2S)$ suppression in p-Pb collisions at $\sqrt{s_{\rm NN}} =$ 5.02 TeV, J. High Energy Phys. 06 (2016) 050.

[58] A. Adare *et al.* (PHENIX Collaboration), Measurement of the relative yields of $\psi(2S)$ to $\psi(1S)$ mesons produced at forward and backward rapidity in $p + p$, $p +$ Al, $p +$ Au, and ^{3}He + Au collisions at $\sqrt{s_{\rm NN}} = 200$ GeV, Phys. Rev. C **95**, 034904 (2017).

[59] A. M. Sirunyan *et al.* (CMS Collaboration), Measurement of prompt and nonprompt J/ψ production in pp and pPb collisions at $\sqrt{s_{\rm NN}} = 5.02$ TeV, Eur. Phys. J. C **77**, 269 (2017).

[60] R. Aaij *et al.* (LHCb Collaboration), Prompt and nonprompt J/ψ production and nuclear modification in pPb collisions at $\sqrt{s_{\rm NN}} = 8.16$ TeV, Phys. Lett. B **774**, 159 (2017).

[61] A. Andronic *et al.*, Heavy-flavour and quarkonium production in the LHC era: from proton-proton to heavy-ion collisions, Eur. Phys. J. C **76**, 107 (2016).

[62] J. P. Lansberg, Theory status of quarkonium production in proton-nucleus collisions, J. Phys. Conf. Ser. **668**, 012019 (2016).

[63] J. J. Aubert *et al.* (European Muon Collaboration), Measurements of the nucleon structure functions $F2_n$ in deep inelastic muon scattering from deuterium and comparison with those from hydrogen and iron, Nucl. Phys. **B293**, 740 (1987).

[64] S. Gavin and R. Vogt, J/ψ Suppression from hadron-nucleus to nucleus-nucleus collisions, Nucl. Phys. **B345**, 104 (1990).

[65] K. Kovařík, A. Kusina, T. Ježo, D. B. Clark, C. Keppel, F. Lyonnet, J. G. Morfín, F. I. Olness, J. F. Owens, I. Schienbein, and J. Y. Yu, nCTEQ15—Global analysis of nuclear parton distributions with uncertainties in the CTEQ framework, Phys. Rev. D **93**, 085037 (2016).

[66] E. J. Eichten and C. Quigg, Mesons with beauty and charm: Spectroscopy, Phys. Rev. D **49**, 5845 (1994).

[67] E. J. Eichten and C. Quigg, Quarkonium wave functions at the origin, Phys. Rev. D **52**, 1726 (1995).

[68] C. Patrignani *et al.* (Particle Data Group), Rev. Part. Phys., Chin. Phys. C **40**, 100001 (2016).

[69] F. Carminati, P. Foka, P. Giubellino, A. Morsch, G. Paic, J.-P. Revol, K. Safarík, Y. Schutz, and U. A. Wiedemann (ALICE Collaboration), ALICE: Physics performance report, volume I, J. Phys. G **30**, 1517 (2004).

[70] B. Alessandro *et al.* (ALICE Collaboration), ALICE: Physics performance report, volume II, J. Phys. G **32**, 1295 (2006).

[71] X. G. Wu, Y. Ma, S. Q. Wang, H. B. Fu, H. H. Ma, S. J. Brodsky, and M. Mojaza, Renormalization group invariance and optimal QCD renormalization scale-setting, Rep. Prog. Phys. **78**, 126201 (2015).

[72] X. G. Wu, S. J. Brodsky, and M. Mojaza, The renormalization scale-setting problem in QCD, Prog. Part. Nucl. Phys. **72**, 44 (2013).